Eph and NMDA receptors control Ca^{2+}/calmodulin-dependent protein kinase II activation during *C. elegans* oocyte meiotic maturation

Chad Corrigan, Rajani Subramanian and Michael A. Miller*

Department of Cell Biology, University of Alabama at Birmingham, Birmingham, AL 35294, USA
*Author for correspondence (e-mail: mamiller@uab.edu)

Summary

Fertilization in the female reproductive tract depends on intercellular signaling mechanisms that coordinate sperm presence with oocyte meiotic progression. To achieve this coordination in *Caenorhabditis elegans*, sperm release an extracellular signal, the major sperm protein (MSP), to induce oocyte meiotic maturation and ovulation. MSP binds to multiple receptors, including the VAB-1 Eph receptor protein-tyrosine kinase on oocyte and ovarian sheath cell surfaces. Canonical VAB-1 ligands called ephrins negatively regulate oocyte maturation and MPK-1 mitogen-activated protein kinase (MAPK) activation. Here, we show that MSP and VAB-1 regulate the signaling properties of two Ca^{2+} channels that are encoded by the NMR-1 N-methyl D-aspartate type glutamate receptor subunit and ITR-1 inositol 1,4,5-triphosphate receptor.

Ephrin/VAB-1 signaling acts upstream of ITR-1 to inhibit meiotic resumption, while NMR-1 prevents signaling by the UNC-43 Ca^{2+}/calmodulin-dependent protein kinase II (CaMKII). MSP binding to VAB-1 stimulates NMR-1-dependent UNC-43 activation, and UNC-43 acts redundantly in oocytes to promote oocyte maturation and MAPK activation. Our results support a model in which VAB-1 switches from a negative regulator into a redundant positive regulator of oocyte maturation upon binding to MSP. NMR-1 mediates this switch by controlling UNC-43 CaMKII activation at the oocyte cortex.

Key words: Major sperm protein, Oocyte maturation, Eph receptor, NMDA receptor, Ca^{2+}/calmodulin-dependent protein kinase II, Inositol triphosphate receptor, Fertilization

Introduction

Meiosis is an essential process that generates haploid (1N) gametes. Although sperm proceed through the meiotic divisions without interruption, the oocytes of most animals arrest during the first prophase (Masui, 1985; Masui and Clarke, 1979). Fertilization and restoration of the diploid chromosome content (2N) depend on signaling mechanisms that coordinate oocyte meiotic progression with sperm presence in the female reproductive tract. In humans, aberrant regulation of the first oocyte meiotic division is a major cause of infertility, miscarriage and chromosomal nondisjunction (Hassold and Hunt, 2001). During this division, oocytes undergo an extended arrest in prophase that can last for years. Pituitary-derived hormones called gonadotropins stimulate the resumption of meiosis through a process called oocyte meiotic maturation, which prepares the oocyte for fertilization and embryogenesis (Hunt and LeMaire-Adkins, 1998). How gonadotropins trigger oocyte maturation in the ovary is not clear, but it may involve antagonism of an inhibitory mechanism(s) imposed by the surrounding follicular cells (Eppig, 2001; Pincus and Enzmann, 1935).

We are using the nematode *Caenorhabditis elegans* as a model with which to investigate the molecular mechanisms by which intercellular signals regulate oocyte meiotic maturation. Oocyte development and fertilization occur in an assembly line fashion within two U-shaped gonad arms that are connected to a common uterus (Hubbard and Greenstein, 2000). Oocytes in diakinesis of meiotic prophase are located in the proximal gonad arm adjacent to the sperm storage compartment, or spermatheca (Fig. 1A) (McCarter et al., 1999). Somatic myoepithelial sheath cells surround the developing oocytes and form gap junctions with them (Hall et al., 1999). Sperm promote oocyte maturation and sheath contraction, which together facilitate ovulation (McCarter et al., 1999). Fertilization occurs as ovulating oocytes enter the spermatheca (Ward and Carrel, 1979). In the absence of sperm, oocytes can arrest in meiotic prophase for days. Because the *C. elegans* hermaphrodite gonad produces roughly 300 sperm prior to oogenesis, oocyte maturation and ovulation occur constitutively in adults until sperm are depleted. In mutant hermaphrodites that do not generate sperm (i.e. females), and in closely related nematode species with separate male and female sexes, oocytes arrest in meiotic prophase until insemination occurs and sperm crawl to the spermatheca (Hill and L'Hernault, 2001).

C. elegans sperm release an extracellular signal, the major sperm protein (MSP), to promote oocyte maturation, MPK-1 mitogen-activated protein kinase (MAPK) activation and sheath contraction (Fig. 1A) (Miller et al., 2001). MSP is the major cytoskeletal element in the sperm pseudopod, where it

functions as an actin analog during amoeboid locomotion (Bottino et al., 2002). MSP leads a dual life as it is also exported from the sperm cytoplasm into the proximal gonad by a membrane-budding mechanism (Kosinski et al., 2005). Extracellular MSP binds to the VAB-1 Eph receptor protein-tyrosine kinase (RPTK) on oocyte and sheath cell surfaces (Miller et al., 2003). Eph RPTKs comprise an evolutionarily conserved receptor class that binds to ligands called ephrins, and the *C. elegans* genome encodes three ephrins that bind to VAB-1 (Chin-Sang et al., 1999; Wang et al., 1999). Ephrin/VAB-1 signaling in oocytes negatively regulates oocyte maturation and MPK-1 MAPK activation (Miller et al., 2003). This pathway acts in parallel to a sheath cell-dependent inhibitory pathway requiring the CEH-18 POU-class homeoprotein (Miller et al., 2003). MSP binding to VAB-1 and an unidentified receptor(s) antagonizes ephrin/VAB-1 and CEH-18-dependent inhibition, resulting in oocyte maturation and MAPK activation (Miller et al., 2003). MSP binds to VAB-1 on sheath cells to stimulate contraction (Miller et al., 2003).

Previously, we have reported that genetic regulators of oocyte meiotic maturation and sheath contraction, including *vab-1* and 28 *msp* loci, are physically clustered in the *C. elegans* genome (Miller et al., 2004). Building on this discovery, we now show that three clustered genes encoding proteins involved in Ca^{2+}-mediated signaling function in the MSP signal transduction mechanism. Our results support a model in which VAB-1 undergoes a switch from negative to positive regulation of oocyte maturation upon binding to MSP.

Materials and methods

C. elegans genetics and strains

Culture and genetic manipulations were carried out as previously described (Brenner, 1974). All *fog-2(q71)* strains were maintained as male/female stocks, while *fog-3(q443)* strains were balanced with the translocation *hT2(qIs48)I*. Strain construction and marker scoring were carried out essentially as previously described, using PCR and phenotypic analyses (Miller et al., 2003). The following strains were used: JK816 [*fem-3(q20)IV*], PD8488 [*rrf-1(pk1417)I*], DG1743 [*fog-3(q443)/hT2(qIs48)I*], DG1744 [*rrf-1(pk1417) fog-3(q443)/hT2(qIs48)I*], CB2 [*vab-1(e2)III*], CZ337 [*vab-1(dx31)II*], DG1612 [*vab-1(dx31)/mIn1II; fog-2(q71)V*], DG1650 [*vab-1(dx31)/mIn1II; fog-2(q71)V; ceh-18(mg57)X*], CB4108 [*fog-2(q71)V*], DG1604 [*fog-2(q71)V; ceh-18(mg57)X*], GR1034 [*ceh-18(mg57)X*], CZ252 [*itr-1(n2559)/lin-45(n2018) unc-24(e138)IV*], JT73 [*itr-1(sa73)IV*], PS2582 [*itr-1(sy290) unc-24(e138)IV*], CB138 [*unc-24(e138)IV*], MM1000 [*itr-1(sa73)IV; fog-2(q71)V*], MM1001 [*itr-1(sy290) unc-24(e138)IV; fog-3(q443)/hT2(qIs48)I*], MM1002 [*vab-1(dx31)II; itr-1(sy290) unc-24(e138)IV*], VM487 [*nmr-1(ak4)II*], CZ793 [*vab-1(e2027)II; lin-15(n765ts)X; juIs24(vab-1::gfp + lin-15(+))*], *nmr-1(ak4)II; lin-15(n765ts)X; Ex61(gfp::nmr-1 + lin-15(+))* (Brockie et al., 2001), MM1003 [*nmr-1(ak4)II; fog-2(q71)V*], MM1004 [*vab-1(dx31) nmr-1(ak4)/mIn1II*], CB408 [*unc-43(e408)IV*], MT1092 [*unc-43(n498)IV*], MT2605 [*unc-43(n1186)IV*], MM1005 [*unc-43(e408)IV; fog-3(q443)/hT2(qIs48)I*], MM1006 [*unc-43(n1186)IV; fog-3(q443)/hT2(qIs48)I*], MM1007 [*unc-43(n498)IV; fog-3(q443)/hT2(qIs48)I*], MM1008 [*unc-43(n498)IV; rrf-1(pk1417) fog-3(q443)/hT2(qIs48)I*], MM1009 [*nmr-1(ak4)II; unc-43(n498)IV*] and MM1010 [*vab-1(dx31)II; unc-43(e408)IV*]. *nmr-1(ak4)* mutants were scored by single worm PCR using the primers AGTGCTGGTGAAGCTCAT and TCCACGTTCTTCAGAAAT, which flank the deletion. The *mIn1II* and *hT2(qIs48)I* balancer

chromosomes are dominantly marked with pharyngeal GFP. *nmr-1(ak4)*, *vab-1(dx31)* and *itr-1(sa73)* heterozygotes were constructed by crossing homozygotes to wild-type or *fog-2(q71)* males. *fem-3(q20)* and *itr-1(sa73)* are temperature-sensitive alleles, and phenotypic studies were carried out at 25°C.

Phenotypic analysis and rate determination

Oocyte meiotic maturation (consisting of nuclear envelope breakdown and cortical cytoskeletal rearrangement), ovulation and ovarian sheath contraction were analyzed in anesthetized animals (0.1% tricaine and 0.01% tetramisole in M9 buffer) on 2% agarose pads as previously described (McCarter et al., 1999). Observation and recording under DIC optics were performed using a Zeiss Axioskop 2 plus, MRM Axiocam Hi-Res digital camera and PC for image acquisition. Oocyte meiotic progression was evaluated by DAPI staining of dissected gonads. For each strain, oocyte maturation and sheath contraction were monitored by direct observation (or time-lapse recording) using DIC optics. Basal sheath contraction rates are measured in adult hermaphrodites and females by monitoring distal migration of the oocyte nuclear envelope, which occurs prior to oocyte maturation and ovulatory contraction. *vab-1(dx31)* is required for basal contraction in adult hermaphrodites and females, but not in young adult hermaphrodites (<30 hours post L4 at 20°C). Oocyte maturation rates were determined by monitoring oocyte ovulations in isolated animals on seeded plates for 4-24 hours. This method was consistent with direct observation by DIC microscopy. Because food is required for high maturation rates, monitoring oocyte ovulations on seeded plates is optimal for accurate quantitation over long time periods (more than 90 minutes). *itr-1(sa73)* has spermathecal valve defects that impair, but do not prevent ovulation and fertilization. In *itr-1(sy290)* gain-of-function females, oocyte maturation rates are slow in young adults (<36 hours post L4), but ovulation rates increase with age. Direct observation by DIC microscopy indicated that spermathecal valve dilation preceded nuclear envelope breakdown in four out of five cases. This defect is probably due to premature spermathecal valve dilation, but it may also be due in part to increased sheath contraction and *unc-43* activation in oocytes. *unc-43(n498)* mutants have vulva defects that inhibit egg laying, so maturation rates were calculated in adults for shorter time periods (2-4 hours). Tables show average oocyte maturation or sheath contraction rates±standard deviation. A two-sample *t*-test was used to test for significance.

RNA-mediated interference

RNAi was performed on L3 or L4 larva by the feeding method (Timmons and Fire, 1998). HT115 bacterial feeding strains were obtained from the genome-wide library (Kamath et al., 2003). To confirm that the feeding strains contained the correct genes, we performed PCR on DNA preps using gene specific primers internal to the cloned region. RNAi phenotypes were compared with those of null mutants to determine effectiveness.

Immunocytochemistry and GFP fluorescence

Monoclonal MAPK-YT (Sigma) and anti-phospho-CaM Kinase II (pThr286, Sigma) antibodies were used to stain dissected gonads as previously described (Miller et al., 2001). Briefly, gonads were rapidly dissected in a watch glass in egg-salts solution, and fixed in 2% neutral-buffered paraformaldehyde overnight at 4°C. Following several washes, gonads were incubated with 1 mg/ml BSA in PBS for 2 hours, then with MAPK-YT (1:2000) or CaMKII-pT (1:250) antibodies for 4 hours at room temperature. Anti-mouse FITC-conjugated secondary antibodies were used for detection. Alexa-Fluor 660 phalloidin (Molecular Probes) and DAPI were used to visualize F-actin and DNA, respectively. Expression was examined using a motorized Zeiss Axioskop 2 plus equipped with epi-fluorescence, an MRM Axiocam Hi-Res digital camera and PC computer for image acquisition. To analyze subcellular localization, axial scans were performed, and out-of-focus light was removed with deconvolution

software (Axiovision). GFP expression of transgenic VAB-1::GFP and NMR-1::GFP reporter strains was examined in dissected gonads. Animals were kept in the dark for 24 hours prior to dissection. Dissected gonads were fixed in 1% neutral-buffered paraformaldehyde for 2 hours at 4°C in the dark. Under these conditions, gonadal GFP expression is detectable by camera in ~20% of the gonads. The VAB-1::GFP and GFP::NMR-1 transgenes rescue the germline and/or somatic defects of the corresponding null mutant hermaphrodites. The GFP::NMR-1 transgene does not show complete rescue, probably because expression is not at the wild-type level.

Microinjection

MSP was microinjected into the gonad using a Zeiss Axiovert 200 microscope, hydraulic fine type micromanipulator and Narishige IM-30 microinjector. The least invasive method to introduce agents into the gonad is by injecting through the vulva into the uterus. Injected animals were anesthetized and mounted for direct observation of the gonad by DIC microscopy.

MSP purification and binding

MSP-6His was purified from *E. coli* under native conditions using Ni-NTA agarose (Qiagen) (Miller et al., 2001). MSP concentrations were determined spectrophotometrically using ϵ (275 nM)$=3.29\times10^4$ M^{-1} cm^{-1} or by BCA protein assay (Pierce) (Miller et al., 2001). MSP-6His was conjugated to NHS-Fluorescein and purified as previously described (Miller et al., 2003). Binding assays were performed in watch glasses following gonad dissection. Briefly, dissected gonads were incubated with MSP-FITC in egg-salts for 20 minutes at room temperature, washed twice with 1 ml egg-salts and fixed with 1% neutral-buffered paraformaldehyde for 10 minutes. MSP-FITC is biologically active, binding to gonads is specific and binding sites are saturated at concentrations greater than 50 nM. MSP-FITC binding can be out-competed with an excess of unlabelled MSP, and BSA-FITC does not bind under the same conditions (Miller et al., 2003). Axial scans of gonads incubated with 25 nM and 100nM MSP-FITC were processed with deconvolution and 3D reconstruction software (Axiovision).

Results

To further investigate the MSP/VAB-1 signaling mechanism, we considered the following two models (Fig. 1B). MSP binding to VAB-1 blocks ephrin/VAB-1 signaling at the receptor level, essentially inactivating all downstream pathways. Alternatively, the MSP/VAB-1 interaction triggers a switch from negative to positive regulation, resulting in downstream events that antagonize ephrin/VAB-1 signaling in the oocyte cytosol. Support for the 'switch' hypothesis comes from studies of vertebrate Eph receptors, which can mediate opposing actions in response to different levels of ephrin activation (Pasquale, 2005; Poliakov et al., 2004). To test the block versus switch models, we decided to characterize downstream effectors of MSP and VAB-1 signaling. Based on physical location in the genome, the *itr-1* inositol 1,4,5-triphosphate (IP$_3$) receptor (Baylis et al., 1999; Dal Santo et al., 1999), *nmr-1* NMDA-type glutamate receptor subunit (Brockie et al., 2001) and *unc-43*
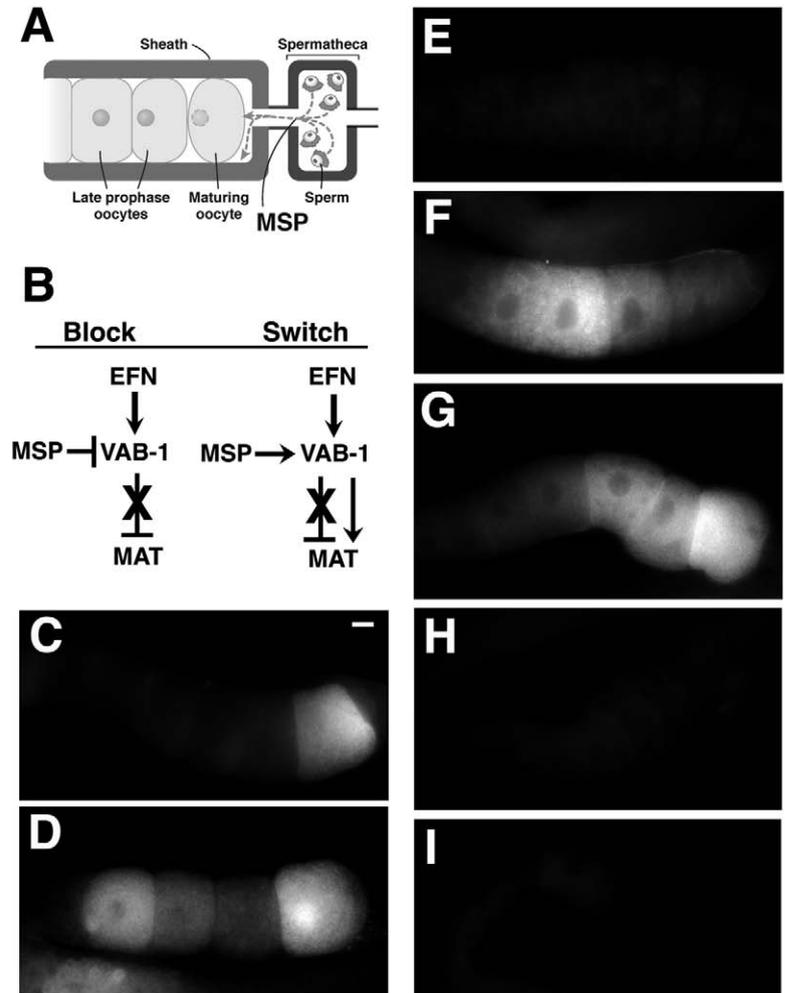

Fig. 1. Models and MPK-1 MAPK activation. (A) In the proximal gonad, somatic ovarian sheath cells surround the oocytes, which are in diakenesis of meiotic prophase. Sperm are stored in the spermatheca and export the cytoskeletal protein MSP to induce oocyte meiotic maturation, MPK-1 MAPK activation and sheath contraction. The maturing oocyte signals the dilation of the spermathecal valve, and the oocyte is fertilized as it enters the spermatheca. (B) Simplified depiction of the block versus switch models for the control of oocyte maturation (MAT). See text for details. (C-I) MAPK-YT staining of wild-type and mutant gonads. (C) In wild-type gonads, sperm trigger MPK-1 MAPK activation in the oocyte(s) most proximal to the spermatheca. (D) In *itr-1(sa73)* hermaphrodites, more oocytes contain activated MAPK than in the wild type. (E) MAPK activation is not observed in unmated *fog-3(q443)* females. (F) By contrast, MAPK activation is frequently observed in unmated *unc-43(n498gf); fog-3(q443)* females. (G) More oocytes contain activated MAPK in *vab-1(dx31)* hermaphrodites, a phenotype identical to *itr-1(sa73)* hermaphrodites (D). (H) In *itr-1(sy290gf) unc-24(e138)* hermaphrodites, fewer oocytes contain activated MAPK than control hermaphrodites. (I) The MAPK activation frequency in *vab-1(dx31); itr-1(sy290gf) unc-24(e138)* hermaphrodites is similar to *itr-1(sy290gf) unc-24(e138)* hermaphrodites, suggesting that *itr-1* acts downstream of *vab-1*. All gonads are oriented as shown in A. The MAPK activation pattern in G has previously been reported elsewhere (Miller et al., 2003). Scale bar: 10 μm.

Ca^{2+}/calmodulin-dependent protein kinase II [CaMKII; (Reiner et al., 1999)] were identified as candidate effectors (Miller et al., 2004).

itr-1 negatively regulates oocyte maturation

A given gene could function as a negative regulator of oocyte maturation, a positive regulator, or both. The latter possibility is indicative of a switch mechanism (Fig. 1B). Negative regulators are identified by using *fog-2(q71)* and *fog-3(q443)* null mutations that eliminate sperm production in hermaphrodites (Ellis and Kimble, 1995; Schedl and Kimble, 1988). To test whether the *itr-1* IP$_3$ receptor negatively regulates oocyte maturation, we constructed *itr-1(sa73); fog-2(q71)* mutants. The *sa73* hypomorphic allele was used for most experiments because *itr-1* is required in spermathecal cells for valve dilation (Clandinin et al., 1998) and *itr-1(n2559)* null mutants do not ovulate. The maturation rate of unmated *itr-1(sa73); fog-2(q71)* females is significantly faster than unmated *fog-2(q71)* controls (Table 1, compare lines 2 and 1; *P*<0.001). Similar results are observed in unmated *itr-1* RNAi *fog-3(q443)* females (Table 1, compare lines 4 and 3; *P*<0.001). To examine oocyte MPK-1 MAPK activation, we used the MAPK-YT antibody, which recognizes the diphosphorylated or activated form of the *mpk-1* gene product (Miller et al., 2001). The average number of stained oocytes per gonad (MAPK activation frequency) in unmated *itr-1(sa73); fog-2(q71)* females is slightly higher than unmated *fog-2(q71)* controls (see Table S1 in the supplementary material, compare lines 2 and 1). These defects are similar to those of *efn-2* and *vab-1* mutants, which synergize with *ceh-18(mg57)*-null mutants (Miller et al., 2003). We conclude that *itr-1* negatively regulates oocyte maturation in the absence of sperm.

Table 1. Oocyte maturation rates

Genotype	Sperm (Y/N)	Maturations per hour	n
1. *fog-2(q71)*	N	0.12±0.09	20
2. *itr-1(sa73); fog-2(q71)*	N	0.45±0.15	11
3. *fog-3(q443)*	N	0.14±0.10	9
4. *itr-1* RNAi *fog-3(q443)*	N	0.50±0.23	8
5. Wild type	Y	2.41±0.40	15
6. *itr-1(sa73)*	Y	1.91±0.24	11
7. *unc-24(e138)*	Y	2.40±0.40	8
8. *itr-1(sy290gf) unc-24(e138)*	Y	1.20±0.31	15
9. *itr-1(sy290gf) unc-24(e138); fog-3(q443)**	N	0.23±0.11	9
10. *rrf-1(pk1417) fog-3(q443)*	N	0.12±0.10	9
11. *itr-1* RNAi *rrf-1(pk1417) fog-3(q443)*	N	0.55±0.20	10
12. *nmr-1(ak4); fog-2(q71)*	N	1.10±0.38	14
13. *nmr-1* RNAi *fog-3(q443)*	N	0.91±0.35	8
14. *nmr-1(ak4)/+; fog-2(q71)*	N	0.72±0.25	12
15. *nmr-1* RNAi *rrf-1(pk1417) fog-3(q443)*	N	0.93±0.33	10
16. *nmr-1(ak4)*	Y	2.13±0.36	14
17. *unc-43(e408); fog-3(q443)*	N	0.10±0.18	13
18. *unc-43(n1186); fog-3(q443)*	N	0.06±0.05	9
19. *unc-43(e408)*	Y	1.22±0.41	12
20. *unc-43(n1186)*	Y	1.46±0.50	8
21. *unc-43(n498gf); fog-3(q443)*	N	0.69±0.25	13
22. *unc-43(n498gf)*	Y	0.63±0.23	8
23. *unc-43* RNAi *unc-43(n498gf); rrf-1(pk1417) fog-3(q443)*	N	0.16±0.17	11
24. *unc-43(n498gf); rrf-1(pk1417) fog-3(q443)*	N	0.67±0.20	10
25. *unc-43* RNAi *unc-43(n498gf); fog-3(q443)*	N	0.18±0.24	10

See text for details. Average value±s.d. is shown.

All alleles are loss of function, unless otherwise noted as gain of function (gf).

*Maturation does occur with increased frequency in older mutant females; however, in four out of five cases that were directly observed, spermathecal valve dilation preceded nuclear envelope breakdown, indicative of a valve defect.

To investigate *itr-1* function in the presence of MSP, we examined *itr-1* mutant hermaphrodites. Nuclear envelope breakdown and progression from diakinesis to metaphase occur normally in *itr-1(sa73)*- and *itr-1(n2559)*-null mutants, and the maturation rate of *itr-1(sa73)* hermaphrodites is close to the wild-type rate (Table 1, compare lines 6 and 5). MPK-1 activation is observed in more oocytes of *itr-1(sa73)* hermaphrodite gonads than wild-type gonads (Fig. 1C,D; see Table S1 in the supplementary material, compare lines 4 and 3; *P*<0.01). This defect is similar to that of *efn-2* and *vab-1* mutants (Miller et al., 2003) (see below). If *itr-1* functions as a negative regulator, then excess *itr-1* activation in the presence of MSP is predicted to slow the oocyte maturation rate. To test this prediction, we examined the *itr-1* gain-of-function allele *sy290gf*, which alters a conserved arginine codon in the IP$_3$-binding domain (Clandinin et al., 1998). Mutation of the homologous residue in the mouse enhances IP$_3$ binding in vitro (Yoshikawa et al., 1996). The maturation rate of *itr-1(sy290gf) unc-24(e138)* hermaphrodites is significantly slower than the rates of *unc-24(e138)* and wild-type hermaphrodites (Table 1, compare lines 8, 7 and 5; *P*<0.001). In addition, the oocyte MAPK activation frequency of *itr-1(sy290gf) unc-24(e138)* hermaphrodites is significantly lower than the controls (Table S1, compare lines 6, 5 and 3; *P*<0.01). The maturation rate of young adult unmated *itr-1(sy290gf) unc-24(e138); fog-3(q443)* females is slow (Table 1, line 9), resembling the rate of unmated *fog-3(q443)* females (Fig. 2; Table 1, line 3). Oocyte MAPK activation is rarely observed in unmated *itr-1(sy290) unc-24(e138); fog-3(q443)* females, at a frequency similar to unmated *fog-3(q443)* controls (Table S1, compare lines 8 and 7). These results support the hypothesis that MSP antagonizes *itr-1* signaling to promote maturation and MPK-1 MAPK activation.

To test for site of action in the gonad, we use *rrf-1(pk1417)* mutants, which are resistant to RNAi in the soma, but sensitive to RNAi in the germ line (Sijen et al., 2001). Using this method, *vab-1* acts in the germ line to inhibit oocyte maturation (Miller et al., 2003). The maturation rates of unmated *itr-1* RNAi *fog-3(q443)* and unmated *itr-1* RNAi *rrf-1(pk1417) fog-3(q443)* females are significantly faster than unmated *fog-3(q443)* and *rrf-1(pk1417) fog-3(q443)* controls (Table 1, compare lines 4, 11 and 3,10; *P*<0.001). Similarly, the MAPK activation frequencies of *itr-1* RNAi wild-type and *itr-1* RNAi *rrf-1(pk1417)* hermaphrodites are significantly higher than wild-type and *rrf-1(pk1417)* hermaphrodites (Table S1, compare lines 10 and 11, and lines 3 and 9; *P*<0.01). We conclude that *itr-1* acts in the germ line to inhibit maturation and MPK-1 MAPK activation.

nmr-1 negatively regulates oocyte maturation in the absence of MSP

The NMR-1 NMDA receptor subunit is most similar to the NR1 family of mammalian subunits (Brockie et al., 2001). To test whether *nmr-1* negatively regulates oocyte maturation, we constructed *nmr-1(ak4); fog-2(q71)* mutants. The *ak4* allele deletes the predicted pore-forming and ligand-binding regions, and is probably a null mutation (Brockie et al., 2001). The oocyte maturation rate of unmated *nmr-1(ak4); fog-2(q71)* females is significantly faster than unmated *fog-2(q71)* females (Table 1, compare lines 12 and 1; *P*<0.001). Similar results are

observed in unmated *nmr-1* RNAi *fog-3(q443)* females (Table 1, compare lines 13 and 3). The MAPK activation frequency of unmated *nmr-1(ak4); fog-2(q71)* females is significantly higher than unmated *fog-2(q71)* controls (Table S1, compare lines 12 and 1; *P*=0.001). These results indicate that *nmr-1* is a negative regulator of maturation and of MAPK activation in the absence of sperm. *nmr-1* is haploinsufficient for this function, as the maturation rate of unmated *nmr-1(ak4)/+; fog-2(q71)* females is significantly faster than unmated *fog-2(q71)* females (Table 1, compare lines 14 and 1; *P*<0.001). To test whether *nmr-1* is required in germ line or somatic cells of the gonad, we used *rrf-1(pk1417) fog-3(q443)* females. The maturation rates of unmated *nmr-1* RNAi *fog-3(q443)* and unmated *nmr-1* RNAi *rrf-1(pk1417) fog-3(q443)* females are significantly faster than unmated *fog-3(q443)* and unmated *rrf-1(pk1417) fog-3(q443)* females (Table 1, compare lines 13 and 15, and lines 3 and 10; *P*<0.001). Therefore, *nmr-1* acts in the germ line to inhibit oocyte maturation.

We examined *nmr-1(ak4)* hermaphrodites and mated females to investigate NMR-1 function in the presence of MSP. Nuclear envelope breakdown, cortical cytoskeletal rearrangement, spermathecal valve dilation and MAPK activation (Table S1, compare lines 13 and 3; *P*>0.10) occur normally in *nmr-1(ak4)* mutants. The oocyte maturation rates of *nmr-1(ak4)* hermaphrodites and mated *nmr-1(ak4); fog-2(q71)* females are close to the wild-type rate (Table 1, compare lines 16 and 5; data not shown), indicating that *nmr-1* does not function as a maturation inhibitor in the presence of sperm. Although NMR-1 is not required to promote oocyte maturation, it may have a redundant function in transducing the MSP signal (see below).

unc-43 is a positive regulator of oocyte maturation

To test whether *unc-43* CaMKII negatively regulates oocyte maturation, we examined females containing the *e408* loss-of-function and *n1186*-null mutations of *unc-43* (Reiner et al., 1999). The oocyte maturation rates of unmated *unc-43(e408); fog-3(q443)* and *unc-43(n1186); fog-3(q443)* females are not significantly different from the rate of unmated *fog-3(q443)* controls (Table 1, compare lines 17, 18 and 3; *P*>0.10), nor are the MAPK activation frequencies different from controls (Table S1, compare line 14 and 7; *P*>0.10). We conclude that *unc-43* is not a negative regulator of oocyte maturation or of MAPK activation.

The maturation rates of *unc-43(e408)* and *unc-43(n1186)* null hermaphrodites are slightly slower than the wild-type rate, raising the possibility that *unc-43* is a positive regulator (Table 1, compare lines 19, 20 and 5; *P*<0.001). Mating *unc-43* mutants with wild-type males does not cause an increase in the maturation rate, demonstrating that this defect is not due to *unc-43* mutant sperm (data not shown). Nuclear envelope breakdown, cortical cytoskeletal rearrangement, MAPK activation and progression to metaphase occur normally in *unc-43(e408)* and *unc-43(n1186)* hermaphrodites (Table S1, line 15). To test whether *unc-43* is a redundant positive regulator of maturation, we examined the gain-of-function allele *n498gf*, which results from an E108K mutation in the kinase domain (Reiner et al., 1999). The maturation rate of unmated *unc-43(n498gf); fog-3(q443)* females is significantly faster than unmated *fog-3(q443)* females (Fig. 2), but it is not significantly different from *unc-43(n498gf)* hermaphrodites [Table 1, compare lines 21 and 3 (*P*<0.001), and lines 21 and 22 (*P*>0.10)]. Therefore, oocyte maturation occurs constitutively independent of sperm in *unc-43(n498gf)* gonads. The maturation rate of *n498gf* mutants is slower than the wild-type rate, owing at least in part to neuronal defects that cause paralysis and prevent egg laying. To test whether *unc-43* activation is sufficient to promote MPK-1 MAPK activation, we stained unmated *unc-43(n498gf)* females with the MAPK-YT antibody. The MAPK activation frequency of unmated *unc-43(n498gf); fog-3(q443)* females is significantly higher than unmated *fog-3(q443)* females [Fig. 1E,F; Table S1, compare lines 16 and 7 (*P*<0.01)]. These results show that *unc-43* is a redundant positive regulator of oocyte maturation and MPK-1 MAPK activation.

To determine the site of *unc-43* action, we constructed *unc-43(n498gf); rrf-1(pk1417) fog-3(q443)* mutants. The
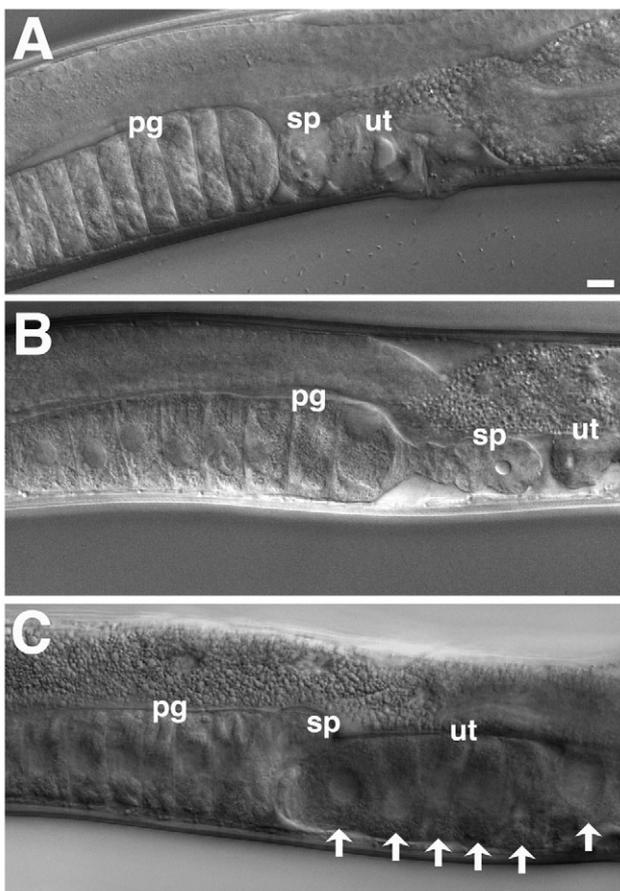

Fig. 2. DIC micrographs of *itr-1* and *unc-43* gain-of-function female gonads. (A) In unmated *fog-3(q443)* female gonads, the oocyte maturation rate is slow and prophase-arrested oocytes accumulate in the proximal gonad (pg) to the left of the spermatheca (sp). Few oocytes that have completed maturation and ovulation are observed in the uterus (ut; no oocytes are seen in A). (B) The maturation rate of young unmated *itr-1(sy290gf) unc-24(e138); fog-3(q443)* females is slow and their gonads resemble young unmated *fog-3(q443)* females. (C) In contrast to unmated *itr-1(sy290gf)* and control females, the maturation rate of young unmated *unc-43(n498gf); fog-3(q443)* females is high. Numerous oocytes that have recently completed maturation and ovulation are observed in the uterus (arrows). Scale bar: 20 μm.

maturation rate of unmated *unc-43* RNAi *unc-43(n498gf); rrf-1(pk1417) fog-3(q443)* females is significantly slower than the rates of unmated *unc-43(n498gf); fog-3(q443)* and *unc-43(n498gf); rrf-1(pk1417) fog-3(q443)* females (Table 1, compare lines 22, 23 and 24; $P<0.001$), but it is not significantly different from the rate of unmated *unc-43* RNAi *unc-43(n498gf); fog-3(q443)* females (Table 1, cf lines 23 and 25; $P>0.10$). We conclude that *unc-43* is required in the germ line to promote maturation. In summary, genetic and RNAi studies are consistent with *itr-1*, *nmr-1* and *unc-43* functioning in oocytes as downstream effectors of MSP signaling.

MSP signaling components are expressed at the oocyte cortex

Proximate effectors of MSP and VAB-1 signaling are predicted to localize at or near the oocyte cell surface. A rescuing VAB-1::GFP translational reporter shows GFP expression on oocyte and sheath cell membranes (Miller et al., 2003). In deconvolved mid-focal plane images, fluorescence appears particularly enriched at membrane sites between oocytes. To test whether the distribution of MSP-binding sites parallels the distribution of VAB-1, we incubated 25 nM MSP-FITC with dissected gonads as described previously (Miller et al., 2003). MSP-FITC is biologically active and binding to gonads is specific (Miller et al., 2003). Control binding experiments performed by pre-incubating gonads with a 25-fold excess of unlabeled MSP do not show MSP-FITC staining. In deconvolved mid focal plane images, the fluorescent intensity at the interface between oocytes is approximately three times greater than the sheath/oocyte interface (Fig. 3A). Three-

dimensional reconstructions show similar results (Fig. 3B), as do incubations with saturating MSP-FITC concentrations (data not shown). This enrichment pattern is still observed when contacting oocytes are dissected away from the sheath (Fig. 3C). By contrast, MSP-FITC-binding sites are uniformly distributed around the plasma membrane in isolated oocytes (Fig. 3D). Mammalian Eph receptors are recruited to membrane sites between contacting cells in culture (Marston et al., 2003). Our results suggest that VAB-1 and other MSP receptors are enriched at and possibly recruited to plasma membrane sites between oocytes.

ITR-1 has been localized to the adult hermaphrodite germ line, sheath cells and spermathecal cells (Baylis et al., 1999; Clandinin et al., 1998; Yin et al., 2004), but the expression of *nmr-1* and *unc-43* in gonads has not been investigated. To investigate the *nmr-1* expression pattern, we examined a GFP::NMR-1 translational reporter strain (Brockie et al., 2001). In dissected gonads, GFP expression is detectable in oocytes (Fig. 3E-G) and sheath cells (Fig. 3N) of transgenic animals, but not in controls (Fig. 3K-M,O; see Materials and methods). GFP fluorescence co-localizes with F-actin at the oocyte cortex, and it appears enriched at contact sites between the oocytes (Fig. 3E-G). An identical pattern is observed in VAB-1::GFP-expressing gonads (Fig. 3H-J). Therefore, VAB-1 and NMR-1 are expressed at the oocyte surface, where they co-localize with F-actin.

To investigate *unc-43* expression, we incubated gonads with an antibody that recognizes phosphorylated (pT286) rat CaMKII (CaMKII-pT). T286 is the primary autophosphorylation site and its phosphorylation correlates with kinase activation (Colbran, 2004). The rat sequence used

Fig. 3. MSP-binding site distribution and expression of GFP::NMR-1 and VAB-1::GFP in the proximal gonad. (A) Fluorescein-labeled MSP (MSP-FITC) binds to oocytes and sheath cells of proximal gonads. In deconvolved mid-focal plane images, fluorescent intensity is enriched at the oocyte/oocyte interface. (B) A 3D reconstruction of the stack shows similar results. (C) The fluorescent intensity is high at membrane sites between oocytes even when the sheath cells are removed. (D) By contrast, MSP-FITC appears uniformly distributed around the oocyte plasma membrane in isolated oocytes. (E-G) In GFP::NMR-1-expressing gonads, GFP fluorescence is observed at the oocyte plasma membrane (E). Extensive co-localization with F-actin (F) is observed in the merged image (G). (H-J) VAB-1::GFP expressing gonads show a similar pattern of fluorescence. (K-M) GFP fluorescence is not observed in control gonads. (N,O) By focusing on the sheath membrane, GFP fluorescence is detected in the sheath of GFP::NMR-1-expressing gonads (N), but not in control gonads (O). Arrows indicate the sheath cells. All gonads are oriented as shown in Fig. 1A. DAPI is included in E-M. The VAB-1::GFP expression pattern has been reported previously (Miller et al., 2003). Scale bars: 10 μm.
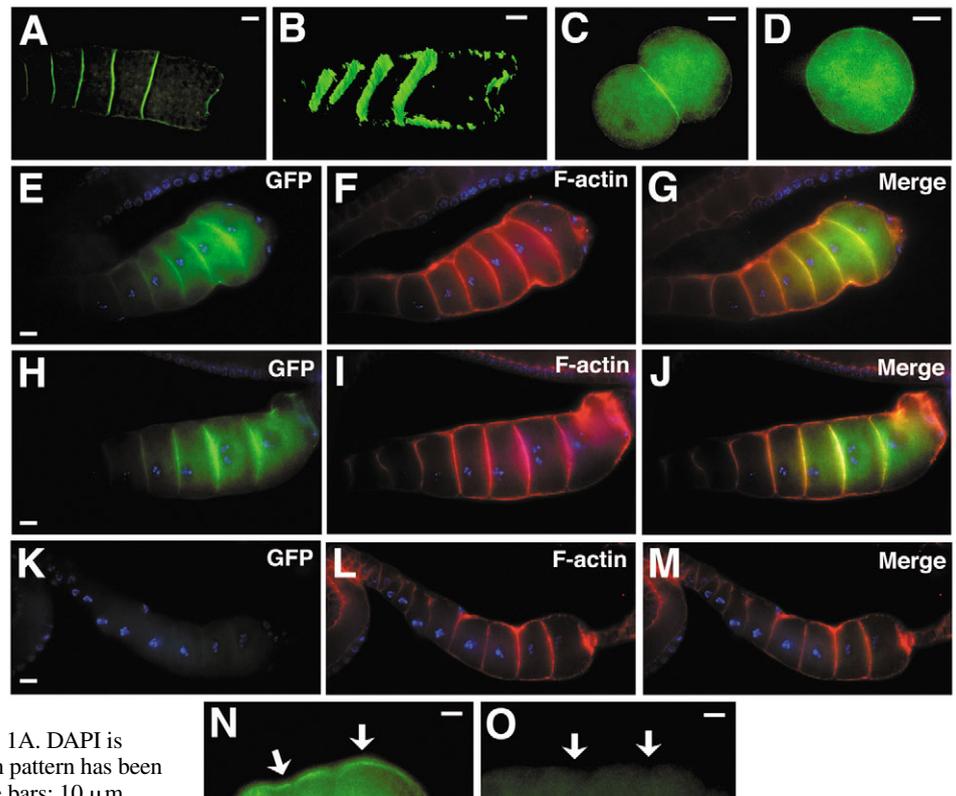
to generate CaMKII-pT is highly conserved in UNC-43, including the phosphorylated threonine (Fig. 4A, T284). The CaMKII-pT antibody stains oocytes of wild-type gonads (Fig. 4B), but not of *unc-43(n1186)* null and *unc-43(e408)* loss-of-function gonads (Fig. 4E; data not shown). Therefore, CaMKII-pT specifically recognizes the *unc-43* gene product. To evaluate the subcellular distribution, we generated a *z*-series through the gonad and processed the images with deconvolution software. Phosphorylated T284 (pT284) UNC-43 co-localizes with F-actin at the oocyte cortex and it is enriched at the oocyte/oocyte interface (Fig. 4B-D), similar to the distribution of GFP::NMR-1 and VAB-1::GFP (Fig. 3E-J). CaMKII-pT staining is also detected at the sheath/oocyte interface of wild-type gonads (Fig. 4H-J). The CaMKII-pT staining pattern contrasts with that of MAPK-YT, which is uniformly distributed throughout the oocyte cytoplasm (Fig. 4K). In wild-type gonads, it is difficult to determine whether UNC-43 is expressed in sheath cells, owing to their close proximity to oocytes and the thinness of the sheath. To test whether pT284 UNC-43 is in sheath cells, we stained *fem-3(q20gf)* mutant gonads with anti-CaMKII-pT. When grown at the restrictive temperature, *fem-3(q20gf)* mutant gonads contain sperm and sheath cells, but not oocytes (Barton et al., 1987). CaMKII-pT stains the somatic cells surrounding sperm in *fem-3(q20gf)* gonads (Fig. 4L). These results indicate that UNC-43 is phosphorylated in sheath cells and in oocytes when sperm are present. In oocytes, pT284 UNC-43 co-localizes with F-actin at the cortex.

CaMKII is activated by Ca^{2+}/calmodulin binding and its activity is further controlled by T286 autophosphorylation, resulting in a Ca^{2+}-independent form (Colbran, 2004; Hook and Means, 2001). The *unc-43(n498gf)* gain-of-function mutation is predicted to result in Ca^{2+}-independent activation (Reiner et al., 1999); however, minimal T284 phosphorylation is observed in *unc-43(n498gf)* gonads (data not shown).
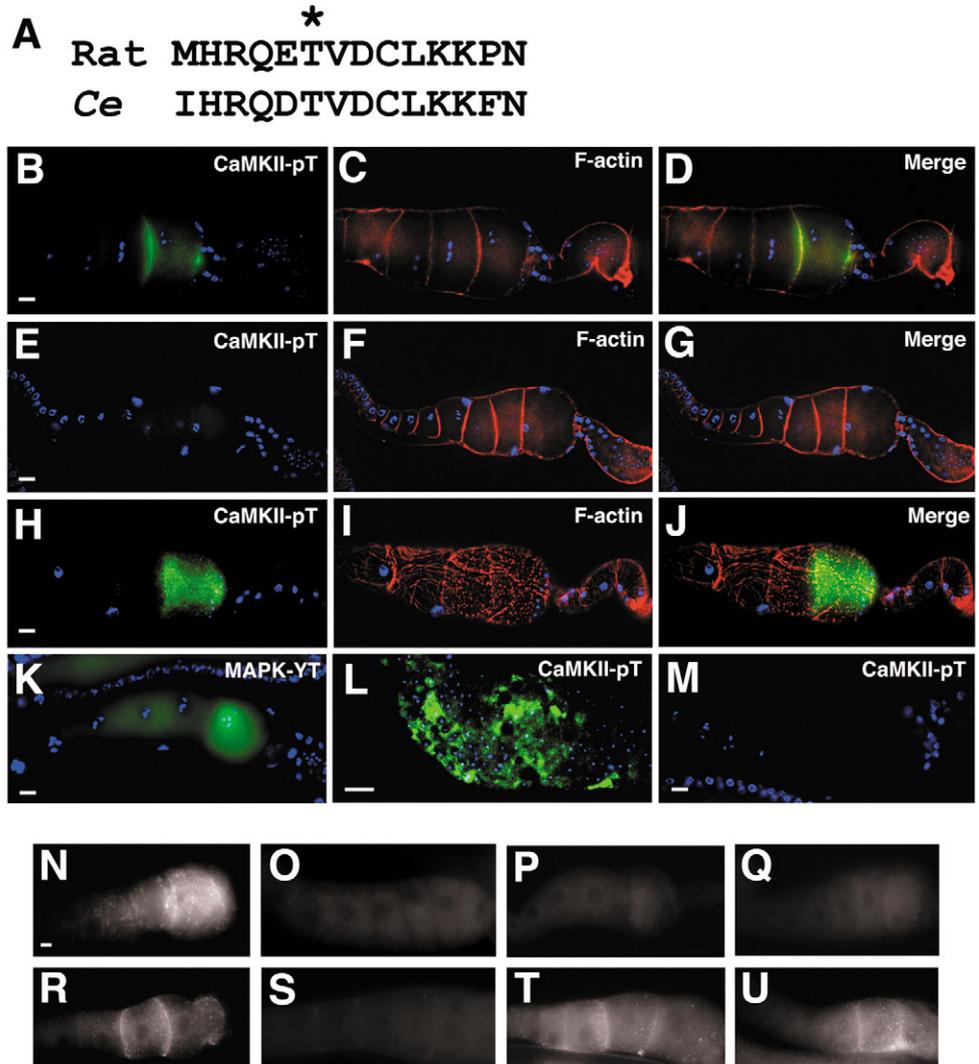

Fig. 4. UNC-43 CaMKII activation in the proximal gonad. (A) The rat sequence used to generate CaMKII-pT is highly conserved in *C. elegans* UNC-43, including the phosphorylated threonine (*, T284 in UNC-43 and T286 in rat CaMKII). (B-D) CaMKII-pT stains the oocytes of wild-type gonads. In mid-focal plane images, staining co-localizes with F-actin at the oocyte cortex. (E-G) CaMKII-pT staining is not observed in *unc-43(n1186)*-null gonads. (H-J) At the sheath and oocyte interface of wild-type gonads, CaMKII-pT staining is observed in the same focal plane as sheath cell F-actin. (K) In contrast to CaMKII-pT, MAPK-YT staining is uniformly distributed throughout the cytoplasm, and sometimes in the nucleus. (L) CaMKII-pT stains sheath cells surrounding the sperm in *fem-3(q20)* gonads. The genetic requirements of UNC-43 T284 phosphorylation are shown in M-U. (M) No CaMKII-pT staining is observed in unmated *fog-3(q443)* females, indicating that sperm are required for UNC-43 T284 phosphorylation. (N,O) CaMKII-pT stains unmated *fog-2(q71)* female gonads microinjected with 100 nM MSP (N), but not buffer-injected control gonads (O). (P) CaMKII-pT staining is not observed in unmated *vab-1* RNAi *ceh-18(mg57)* females, which undergo constitutive oocyte maturation independent of sperm presence. CaMKII-pT staining is not observed in *vab-1(dx31)* (Q) and *nmr-1(ak4)* gonads (S), but it is observed in *vab-1(e2)* kinase dead (R), *itr-1(sa73)* (T) and *itr-1(sy290gf)* (U) gonads. All images in B-M were processed with deconvolution software and include DAPI to visualize DNA. All gonads are oriented as shown in Fig. 1A. Scale bars: 10 μm.

CaMKII and many other protein kinases are capable of signaling in the absence of activation loop phosphorylation (Colbran, 2004; Kroiher et al., 2001). Phosphorylation is indicative of kinase activation, but lack of phosphorylation is not necessarily indicative of an inactive state. We conclude that UNC-43 activation does not require T284 phosphorylation and

speculate that T284 phosphorylation results in a Ca^{2+}-independent form.

itr-1 acts downstream of ephrin/vab-1 signaling

The ephrin *efn-2* acts in the germ line together with VAB-1 to negatively regulate oocyte maturation and MPK-1 MAPK activation (Miller et al., 2003). Mutations in the *vab-1* extracellular ephrin-binding domain that disrupt signaling by ephrins cause inhibition defects (Miller et al., 2003). Collectively, previous studies are consistent with multiple ephrins acting through VAB-1 to inhibit maturation in hermaphrodites and unmated females, although reverse signaling is also possible (Pasquale, 2005). Receptor protein-tyrosine kinases are well known stimulators of IP$_3$ production, and IP$_3$ binding to IP$_3$ receptors mobilizes intracellular Ca^{2+}. *efn-2*, *vab-1* and *itr-1* mutants have similar phenotypes in hermaphrodites and unmated females, suggesting that the wild-type genes function in a common pathway [Fig. 1D,G; Table S1, compare lines 17 and 4; Table 2, compare lines 1 and 2; (Miller et al., 2003)]. To determine the genetic relationship between *itr-1* and ephrin/vab-1 signaling, we constructed *vab-1(dx31); itr-1(sy290gf)* hermaphrodites. The oocyte MAPK activation frequency is high in *vab-1(dx31)* and *itr-1(sa73)* gonads (Fig. 1D,G; Table S1, lines 17 and 4) and low in *itr-1(sy290gf)* gonads (Fig. 1H; Table S1, line 6). If *itr-1* acts downstream of *vab-1*, then the double mutants should resemble *itr-1(sy290gf)* mutants. The MAPK activation frequency in *vab-1(dx31); itr-1(sy290gf)* gonads is not significantly different from that of *itr-1(sy290)* gonads (Fig. 1H,I; Table S1, compare lines 18 and 6). In addition, the maturation rate of the double mutants is not significantly different from the rate of *itr-1(sy290gf)* hermaphrodites, but it is significantly slower than *vab-1(dx31)* hermaphrodites (Table 2, compare lines 3, 4 and 5; $P<0.001$). These results indicate that *itr-1* acts

Table 2. Genetic relationships among maturation regulators

Genotype	Sperm (Y/N)	Maturations per hour	n
1. *vab-1(dx31); fog-2(q71)**	N	0.45±0.19	13
2. *itr-1* RNAi *fog-2(q71)*	N	0.53±0.20	7
3. *vab-1(dx31); itr-1(sy290gf) unc-24(e138)*	Y	1.19±0.29	9
4. *itr-1(sy290gf) unc-24(e138)*	Y	1.20±0.31	15
5. *vab-1(dx31)**	Y	2.15±0.44	11
6. *itr-1* RNAi *vab-1(dx31); fog-2(q71)*	N	0.52±0.16	9
7. *unc-43* RNAi *vab-1(dx31); fog-2(q71)*	N	0.49±0.24	8
8. *nmr-1(ak4); fog-2(q71)*	N	1.10±0.38	14
9. *unc-43* RNAi *nmr-1(ak4); fog-2(q71)*	N	0.37±0.18	14
10. *nmr-1(ak4) vab-1(dx31); fog-2(q71)*	N	0.53±0.17	10
11. *itr-1* RNAi *nmr-1(ak4); fog-2(q71)*	N	0.14±0.11	13
12. *itr-1* RNAi *nmr-1(ak4); fog-2(q71)*	Y	1.74±0.51	6
13. *nmr-1(ak4)/+; fog-2(q71)*	N	0.72±0.21	12
14. *vab-1(dx31)/ +; fog-2(q71)*	N	0.09±0.07	9
15. *nmr-1(ak4) vab-1(dx31)/ + +; fog-2(q71)*	N	0.40±0.24	10
16. *itr-1(sa73)/ +; fog-2(q71)*	N	0.14±0.11	5
17. *nmr-1(ak4)/ +; itr-1(sa73)/ +; fog-2(q71)*	N	0.38±0.22	10
18. 100 nM MSP injected into *unc-43(n1186); fog-3(q443)*	N	1.80±0.45	5
19. Control injection into *unc-43(n1186); fog-3(q443)*	N	0.15±0.12	8

See text for details. Average value±s.d. is shown.
All alleles are loss of function, unless otherwise noted as gain of function (gf).
*New data that have been described previously (Miller et al., 2003).

downstream of or in parallel to a *vab-1*-dependent inhibitory pathway. To distinguish between these possibilities, we measured the oocyte maturation rates of unmated *vab-1* RNAi *itr-1(sa73); fog-2(q71)* and *itr-1* RNAi *vab-1(dx31); fog-2(q71)* females. These rates are not significantly different from unmated single mutant controls (Table 2, compare lines 6, 2 and 1; data not shown; $P>0.10$), indicating that *itr-1* does not act in parallel to ephrin/*vab-1* signaling. Furthermore, the *vab-1(ju8)* ephrin-binding domain mutant (Chin-Sang et al., 1999; Wang et al., 1999) does not show an additive phenotype with *itr-1* RNAi ($P>0.10$). Ephrin/VAB-1 signaling acts in parallel to *ceh-18* to inhibit oocyte maturation (Miller et al., 2003). We could not test whether *itr-1* acts in parallel to *ceh-18* because *itr-1* RNAi *ceh-18(mg57)* oocytes mature, but rarely ovulate due to synergistic defects in the somatic gonad. These results support the hypothesis that *itr-1* acts downstream of ephrin/VAB-1 signaling to inhibit oocyte maturation.

nmr-1 inhibits unc-43 signaling in the absence of MSP

If the block model is correct, then loss of ephrin/VAB-1 signaling in unmated females should result in the precocious activation of downstream MSP-responsive positive effectors (maturation promoters). It follows that loss of a downstream positive effector should suppress loss of ephrin/VAB-1 signaling. Genetic analysis indicates that UNC-43 is a redundant positive regulator of oocyte maturation and MPK-1 MAPK activation. To test whether ephrin/VAB-1 signaling negatively regulates UNC-43, we measured the oocyte maturation rate of unmated *unc-43* RNAi *vab-1(dx31); fog-2(q71)* females. The rate of these mutants is not significantly different from unmated *vab-1(dx31); fog-2(q71)* females (Table 2, compare lines 7 and 1; $P>0.10$). In addition, *unc-43* RNAi does not suppress the inhibition defect of *efn-2(ev658)*-null hermaphrodites depleted of sperm ($P>0.10$). Parallel control experiments using *unc-43(n498); fog-3(q443)* and *nmr-1(ak4); fog-2(q71)* females demonstrate that *unc-43* RNAi is disrupting *unc-43* function (see below, Table 2, lines 8 and 9). These results provide strong evidence that ephrin/VAB-1 signaling does not inhibit *unc-43* activity.

Mammalian NMDA receptors bind to and regulate CaMKII activity in cultured neurons (Bayer et al., 2001; Colbran, 2004). To test whether *nmr-1* negatively regulates *unc-43*, we measured the maturation rate of unmated *unc-43* RNAi *nmr-1(ak4); fog-2(q71)* females. Their rate is significantly slower than unmated *nmr-1(ak4); fog-2(q71)* females (Table 2, compare lines 8 and 9; $P<0.001$), indicating that loss of *unc-43* suppresses the inhibition defect of *nmr-1*-null mutants. We conclude that NMR-1 negatively regulates UNC-43 signaling in the absence of sperm. These results appear inconsistent with the block model, but further investigation of the relationship between MSP, VAB-1 and NMR-1 is necessary to draw definitive conclusions.

NMR-1 can control the direction of VAB-1 signaling

The parallel and redundant structure of the MSP signaling mechanism raises the possibility that crosstalk exists among pathways. To investigate the genetic relationship between *nmr-1* and *vab-1* pathways, we constructed *vab-1(dx31) nmr-1(ak4); fog-2(q71)* mutants. The maturation rate of unmated *vab-1(dx31) nmr-1(ak4); fog-2(q71)* females is significantly

slower than unmated *nmr-1(ak4); fog-2(q71)* females (Table 2, compare lines 10 and 8; *P*<0.001), indicating that *vab-1(dx31)* suppresses the *nmr-1(ak4)* inhibitory defect. This relationship suggests that VAB-1 can act in a positive direction to promote oocyte maturation in the absence of NMR-1 and MSP. When NMR-1 is present, VAB-1 acts as a negative regulator. Genetic data support the hypothesis that ITR-1 acts downstream of ephrin/VAB-1 signaling to inhibit oocyte maturation. To test the genetic relationship between *nmr-1* and *itr-1*, we measured the maturation rate of unmated *itr-1* RNAi *nmr-1(ak4); fog-2(q71)* females. The rate is significantly slower than unmated *nmr-1(ak4); fog-2(q71)* females (Table 2, compare lines 11 and 8; *P*<0.001). Moreover, it is not different from unmated *fog-2(q71)* controls (Table 1, line 1), indicating that both *nmr-1* and *itr-1* mutant defects are completely suppressed. Taken together, these results suggest that crosstalk between NMR-1 and VAB-1/ITR-1 pathways controls the direction of downstream signaling. Wild-type sperm stimulate a robust increase in the maturation rates of *itr-1* RNAi *nmr-1(ak4); fog-2(q71)* and *vab-1(dx31) nmr-1(ak4); fog-2(q71)* females (Table 2, line 12 and data not shown). Therefore, this control mechanism must be redundant with another sperm-responsive pathway(s).

Biochemical studies have shown that Eph and NMDA receptors directly interact in cultured mammalian cells, leading to the recruitment of CaMKII (Dalva et al., 2000). Our protein localization data are consistent with NMR-1 and VAB-1 being components of a heteromeric complex. A reduction in *nmr-1* dose is sufficient to trigger oocyte maturation in the absence of sperm (Table 1, line 14). Haploinsufficiency can be indicative of a balance in signaling among components of a protein complex (Papp et al., 2003). To test whether a balance between NMR-1 and VAB-1/ITR-1 signaling is important for regulating maturation, we examined the maturation rates of unmated *vab-1(dx31) nmr-1(ak4)/+ +* and *nmr-1(ak4)/+; itr-1(sa73)/+* females. The rates of the double heterozygotes are significantly slower than the rate of unmated *nmr-1(ak4)/+* females [Table 2, compare lines 15, 14 and 13 (*P*=0.004), and lines 17, 16, and 13 (*P*=0.002)]. We conclude that the level of signaling between NMR-1 and VAB-1 pathways is crucial for the inhibitory response. Collectively, the data suggest that the NMR-1 NMDA receptor subunit can control the direction of VAB-1 signaling.

MSP binding to VAB-1 stimulates NMR-1-dependent UNC-43 activation

UNC-43 is phosphorylated in oocytes and sheath cells when sperm are present (Fig. 4B-J,L). If MSP stimulates UNC-43 activation, then UNC-43 phosphorylation should not occur in the absence of sperm. To test this prediction, we stained unmated *fog-2(q71)* and *fog-3(q443)* females with anti-CaMKII-pT. No staining is observed in the absence of sperm (Fig. 4M). To test whether MSP is sufficient to trigger UNC-43 phosphorylation, we microinjected 100 nM MSP into unmated *fog-2(q71)* females and stained their gonads with CaMKII-pT. pT284 UNC-43 is detected in MSP microinjected gonads, but not in control-injected gonads (Fig. 4N,O). These results support the hypothesis that MSP triggers UNC-43 activation in the gonad. This mechanism must be redundant with another MSP-responsive pathway(s), as 100 nM MSP can promote oocyte maturation when microinjected into unmated *unc-43(n1186); fog-3(q443)* females (Table 2, line 18). Control

injections with buffer alone did not stimulate oocyte maturation (Table 2, line 19). Therefore, MSP stimulates UNC-43-dependent and -independent pathways to promote oocyte maturation.

To test the block versus switch models further, we investigated the genetic requirements of UNC-43 T284 phosphorylation. Ephrin/VAB-1 and CEH-18-dependent signaling act in parallel to inhibit oocyte maturation and MAPK activation (Miller et al., 2003). The block model predicts that T284 phosphorylation should occur in unmated *vab-1* RNAi *ceh-18(mg57)* females, which undergo constitutive oocyte maturation independent of MSP presence (Miller et al., 2003). CaMKII-pT staining is not observed in unmated *vab-1* RNAi *ceh-18(mg57)* females (Fig. 4P). Furthermore, UNC-43 T284 is not phosphorylated in unmated *nmr-1(ak4); fog-2(q71)* and *vab-1(dx31); fog-2(q71)* females (data not shown). We conclude that MSP does not stimulate UNC-43 T284 phosphorylation by simply disrupting VAB-1 or NMR-1 function. These results are not consistent with the block model and suggest that MSP functions as an agonist in promoting UNC-43 activation.

If MSP induces a switch in VAB-1 signaling activity that triggers UNC-43 T284 phosphorylation, then VAB-1 should be required for CaMKII-pT staining in hermaphrodites. Consistent with this prediction, no staining is observed in *vab-1(dx31)* null hermaphrodite gonads (Fig. 4Q). UNC-43 T284 is phosphorylated in *vab-1(e2)* kinase-dead mutants (Fig. 4R), indicating that VAB-1 phosphotransferase activity is not necessary. Ca^{2+} mobilization by mammalian NMDA receptors can stimulate CaMKII T286 phosphorylation in cultured neuronal cells (Bayer et al., 2001; Colbran, 2004). To test whether the *nmr-1* NMDA receptor subunit is required for UNC-43 T284 phosphorylation, we stained *nmr-1(ak4)* hermaphrodites with CaMKII-pT. No staining is observed in *nmr-1(ak4)* gonads (Fig. 4S). By contrast, T284 is phosphorylated in the *itr-1* IP_3 receptor mutants *itr-1(sa73)* (Fig. 4T) and *itr-1(sy290gf)* (Fig. 4U), as well as in *ceh-18(mg57)* mutants (data not shown). These results suggest that MSP promotes UNC-43 T284 phosphorylation by regulating NMDA receptor-dependent Ca^{2+} mobilization. Because MSP and VAB-1 directly interact (Miller et al., 2003) and MSP-FITC binding to oocytes is not reduced in *nmr-1(ak4)* gonads (*P*>0.10), we favor a model in which MSP binding to VAB-1 stimulates NMR-1-dependent UNC-43 T284 phosphorylation and signaling. These results, together with genetic analysis of unmated females, are consistent with a switch mechanism that controls UNC-43 CaMKII activation.

MSP stimulates UNC-43 activation in sheath cells to regulate contraction

For the switch model to be correct, MSP should have signaling properties of an agonist. MSP binding to VAB-1 on sheath cells acts in a positive direction to stimulate contraction. This mechanism does not require ephrins and exhibits less redundancy than the maturation mechanism (Miller et al., 2003). NMR-1 and UNC-43 are expressed in oocytes and sheath cells (Figs 3 and 4), raising the possibility that these cells share a common circuitry that promotes UNC-43 activation. To investigate the role of *nmr-1* and *unc-43* in sheath contraction, we measured the basal contraction rates of mutant and RNAi animals in the presence and absence of sperm. The

Table 3. Sheath contraction rates

Genotype	Sperm (Y/N)	Contractions per min	n
1. Wild type	Y	9.8±1.4	25
2. nmr-1(ak4)	Y	19.1±4.7	10
3. unc-43(n1186)	Y	16.7±2.1	9
4. unc-43(e408)	Y	17.8±4.4	12
5. fog-2(q71)	N	1.9±0.6	19
6. nmr-1(ak4); fog-2(q71)	N	1.4±1.1	10
7. fog-3(q443)	N	1.8±0.9	9
8. unc-43(n1186); fog-3(q443)	N	1.9±1.1	9
9. 100 nM MSP inj fog-2(q71)	N	9.3±1.8	8
10. Buffer inj unc-43(n1186); fog-3(q443)	N	2.2±1.6	5
11. 100 nM MSP inj unc-43(n1186); fog-3(q443)	N	20.3±2.0	7
12. unc-43(n498gf); nmr-1(ak4)	Y	4.7±2.1	11
13. unc-43(n498gf)	Y	5.0±2.0	12
14. vab-1(dx31)*	Y	4.3±1.2	12
15. vab-1(dx31); unc-43(e408)	Y	5.9±1.9	15
16. vab-1(dx31); nmr-1(ak4)	Y	5.2±1.4	12

See text for details. Average value±s.d. is shown.

All alleles are loss of function, unless otherwise noted as gain of function (gf).

*New data that have been described previously (Miller et al., 2003).

contraction rates of *nmr-1(ak4)* and *nmr-1* RNAi hermaphrodites are almost twice the wild-type rate [Table 3, compare lines 2 and 1 (*P*<0.001); see Table S2 in the supplementary material, compare lines 2 and 1]. Similar results are observed in *unc-43(n1186)* null, *unc-43(e403)* and *unc-43* RNAi hermaphrodites [Table 3, compare lines 3, 4 and 1 (*P*<0.001); see Table S2, compare lines 3 and 1). If *nmr-1* and *unc-43* functions are dependent on MSP, contraction defects should not be observed in unmated mutant females. The contraction rates of unmated *nmr-1(ak4); fog-2(q71)* and *unc-43(n1186); fog-3(q443)*-null females are not significantly different from the rates of unmated *fog-2(q71)* and *fog-3(q443)* controls [Table 3, compare lines 6 and 5 (*P*>0.10) and lines 8 and 7 (*P*>0.10)]. We conclude that *nmr-1* and *unc-43* are negative regulators of sperm-dependent sheath contraction. RNAi studies using *rrf-1(pk1417)* and *fem-3(q20)* mutants demonstrate that *nmr-1* and *unc-43* function in the somatic gonad to control sheath contraction (see Table S2 in the supplementary material).

To test whether MSP is sufficient to activate UNC-43 in sheath cells, we microinjected 100 nM MSP into unmated *unc-43(n1186); fog-3(q443)* and *fog-3(q443)* females. The contraction rate of MSP-injected *unc-43(n1186); fog-3(q443)* females is significantly faster than the rate of MSP-injected *fog-3(q443)* females and buffer-injected *unc-43(n1186); fog-3(q443)* females (Table 3, compare lines 9, 10 and 11; *P*<0.001). Therefore, MSP promotes UNC-43 activation in sheath cells, where it attenuates the basal contraction rate.

UNC-43 T284 phosphorylation is not observed in *nmr-1(ak4)* hermaphrodite gonads (Fig. 4S), suggesting that UNC-43 acts downstream of NMR-1 in oocytes and sheath cells. The identical contraction defects of *unc-43* and *nmr-1* mutants are consistent with this relationship (Table 3, compare lines 2-4). To determine the genetic relationship between *unc-43* and *nmr-1*, we examined hermaphrodites containing the *unc-43(n498gf)* gain-of-function allele and *nmr-1(ak4)* null allele. The contraction rate of *unc-43(n498gf); nmr-1(ak4)* mutants is significantly slower than the rate of *nmr-1(ak4)* hermaphrodites (Table 3, compare lines 12 and 2; *P*<0.001), but it is not

significantly different from the rate of *unc-43(n498gf)* hermaphrodites (Table 3, compare lines 12 and 13). These results support the hypothesis that *unc-43* acts downstream on *nmr-1*.

MSP binding to VAB-1 and an unidentified receptor(s) stimulates ITR-1 signaling in sheath cells to promote basal contraction (M.A.M., unpublished) (Yin et al., 2004). If the MSP/VAB-1 interaction stimulates a distinct pathway resulting in UNC-43 activation, then loss of VAB-1 should prevent UNC-43 T284 phosphorylation and signaling. In support of this prediction, T284 is not phosphorylated in *vab-1(dx31)*-null gonads (Fig. 4Q). To test whether *nmr-1/unc-43* signaling is dependent on *vab-1*, we examined *vab-1(dx31); unc-43(e408)* and *vab-1(dx31); nmr-1(ak4)* hermaphrodites. The contraction rates of these double mutants are similar to the rate of *vab-1(dx31)* mutants (Table 3, compare lines 16, 15 and 14), indicating that *unc-43* function is largely dependent on *vab-1*. Genetic analysis of sheath contraction supports the hypothesis that MSP binding to VAB-1 stimulates NMR-1-dependent UNC-43 activation. This mode of action is indicative of an agonist.

Discussion

Here, we characterize downstream effectors of MSP and VAB-1 signaling to test models of the transduction mechanism. Our results support a model in which MSP binding to VAB-1 induces a switch from negative to positive regulation. Activation of vertebrate Eph receptors can lead to cell adhesion or repulsion in migrating neurons, depending on the level of input (Pasquale, 2005; Poliakov et al., 2004). There is also evidence for negative and positive regulation of the MAPK cascade in cultured cells (Pasquale, 2005; Poliakov et al., 2004). Thus, Eph receptors are capable of signaling opposing actions. In the *C. elegans* gonad, the ability to switch from negative to positive regulation could allow hermaphrodites to fine-tune their oocyte maturation rates in response to changing sperm levels. As sperm are depleted from the reproductive tract, MSP-responsive effectors such as UNC-43 CaMKII and MPK-1 MAPK must be downregulated to prevent oocyte meiotic progression and ovulation. Switch mechanisms may confer a selective advantage by conserving metabolically costly oocytes when fertilization is not possible (Miller et al., 2003). Below, we discuss evidence for the switch model in the context of the MSP sperm-sensing mechanism.

Negative regulation in the absence of MSP

The ephrin *efn-2* and *vab-1* function in the germ line to negatively regulate oocyte maturation and MPK-1 MAPK activation in the absence of MSP (Miller et al., 2003). Ephrin/VAB-1 signaling acts in parallel to a sheath cell-dependent pathway requiring the CEH-18 POU-class homeoprotein (Fig. 5A). CEH-18 is required for the assembly or maintenance of sheath/oocyte gap junctions (Rose et al., 1997). Genetic data support the hypothesis that the ITR-1 IP$_3$ receptor acts downstream of ephrin/VAB-1 signaling in oocytes (Fig. 5A). Mammalian ephrins are capable of transducing signals in a 'reverse' direction (i.e. from receptor to ligand) and our current data cannot distinguish between forward and reverse modes of action. However, RPTKs are
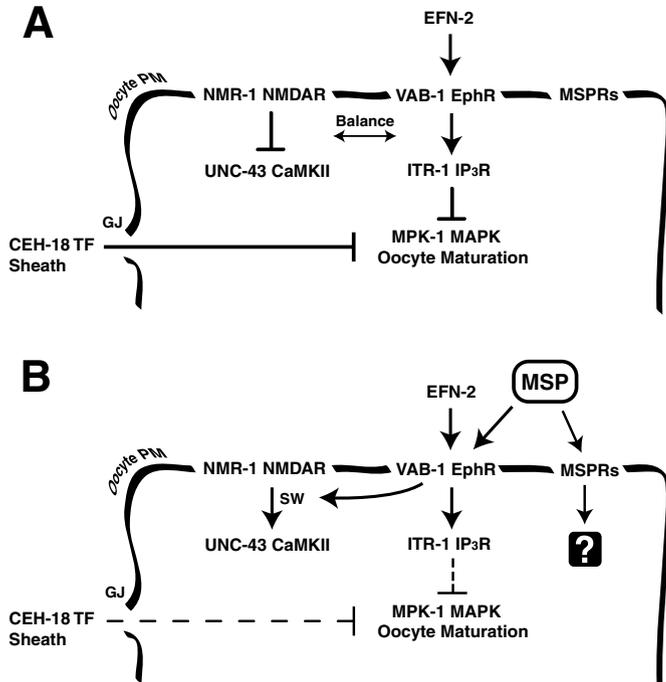
Fig. 5. Working models of the MSP signaling mechanism. MSP binds to multiple receptors on the oocyte plasma membrane (PM), including the VAB-1 Eph receptor. (A) When extracellular MSP is scarce or absent, ephrin/VAB-1- and CEH-18-dependent pathways negatively regulate MPK-1 MAPK activation and oocyte maturation. The ITR-1 IP$_3$ receptor acts downstream of VAB-1, while the NMR-1 NMDA-receptor subunit prevents activation of UNC-43 CaMKII. (B) MSP binding to VAB-1 triggers a switch (SW) from negative to positive regulation. As a result, NMR-1 stimulates UNC-43 T284 phosphorylation and signaling at the oocyte cortex. MSP also binds to unidentified MSP receptors (MSPRs) that act redundantly to promote oocyte maturation. MSPRs could function in oocytes (shown), sheath cells or both. Broken lines indicate downregulated pathways. See text for details. Models are based on results from this study and previous studies. SW, switch; GJ, gap junction; TF, transcription factor; IP$_3$R, inositol triphosphate receptor.

well known stimulators of IP$_3$ production in cultured mammalian cells (Berridge, 1993). In the textbook model, ligand binding induces RPTK dimerization and phospholipase C (PLC) activation. PLC hydrolyzes phosphatidyl 4,5-bisphosphate to IP$_3$, which binds to IP$_3$ receptors and stimulates Ca^{2+} mobilization. Increases in local Ca^{2+} trigger the activation of Ca^{2+}-responsive effectors that modulate the cell cycle and cytoskeleton.

The NMR-1 NMDA-subtype glutamate receptor subunit, a Ca^{2+}-channel component expressed at the oocyte cell surface, negatively regulates oocyte maturation in unmated females. The *nmr-1(ak4)* inhibition defect is suppressed by loss of UNC-43 CaMKII, a positive regulator whose gain-of-function phenotype is constitutive maturation independent of sperm presence. This result indicates that NMR-1 negatively regulates UNC-43 signaling in the absence of MSP (Fig. 5A). The role of glutamate in NMR-1 function in the gonad is not currently known, but the microinjection of glutamate into unmated females does not promote oocyte maturation (M.A.M., unpublished).

The first evidence for a switch mechanism comes from studies of the genetic relationship between NMR-1 and VAB-1 receptor pathways. Loss of *vab-1* or *itr-1* suppresses the inhibition defect of unmated *nmr-1(ak4)*-null mutant females, suggesting that *vab-1* and *itr-1* can act in a positive direction. When *nmr-1* is present, *vab-1* and *itr-1* are negative regulators. One explanation for the data is that NMR-1 can control the direction of VAB-1 signaling. Reducing the *nmr-1* dose is sufficient to trigger oocyte maturation in the absence of sperm, and this defect is partially suppressed by a reduction in *vab-1* or *itr-1* dose. These relationships are indicative of a balance in signaling between VAB-1 and NMR-1 pathways (Fig. 5A). A balanced receptor ratio could prevent the activation of maturation promoting enzymes such as UNC-43 when sperm are not available for fertilization. A shift in the balance might result in precocious activation of these enzymes. The complete loss of inhibition defects in unmated *itr-1* RNAi *nmr-1(ak4)* females suggests that ITR-1 and NMR-1 have inhibitory and promoting activities. Alternatively, other mechanisms may be able to compensate for their inhibitory functions when both genes are inactivated. Further studies will be necessary to completely understand the mechanism by which VAB-1 Eph and NMR-1 NMDA receptor pathways control oocyte maturation in the absence of MSP.

The switch to positive regulation

MSP binding to VAB-1 and an unidentified receptor(s) antagonizes ephrin/VAB-1 and CEH-18-dependent inhibition (Fig. 5B) (Miller et al., 2003). Significant redundancy must exist in this mechanism, as MSP can still promote oocyte maturation in unmated *vab-1* and *unc-43*-null mutant females (Fig. 5). The MSP/VAB-1 interaction could block ephrin/VAB-1 signaling at the receptor level or it could trigger a switch from negative to positive regulation (Fig. 1B). For the switch model to be correct, MSP and VAB-1 must stimulate downstream events that are distinct from those occurring in unmated *vab-1*-null mutant females. These events should be consistent with the action of an agonist, although the overall response is antagonistic. Switch mechanisms might exist in signaling networks composed of interacting hierarchies of negative and positive regulators, as there may be more opportunities during evolution to create inducible transitions. Consistent with such a theoretical argument, some characterized intracellular regulators of *C. elegans* oocyte maturation function as positive regulators, whereas others function as negative regulators (Boxem et al., 1999; Detwiler et al., 2001; Miller et al., 2004).

We show that MSP induces UNC-43 activation in oocytes and sheath cells. Results from two sets of experiments demonstrate that MSP does not promote UNC-43 activation by blocking ephrin/VAB-1 signaling at the receptor level. First, the T284 phosphorylated form of UNC-43 is not observed in unmated *vab-1(dx31)*-null and *vab-1(dx31); ceh-18(mg57)* female gonads; it is observed when MSP is present. Second, loss of UNC-43 does not suppress the inhibition defects of *vab-1-* and *efn-2*-null mutants. These experiments indicate that ephrin/VAB-1 signaling negatively regulates oocyte maturation by a mechanism independent of UNC-43 (Fig. 5A).

To determine whether MSP acts as an agonist in promoting UNC-43 activation, we sought to identify gene products that regulate this event. Both VAB-1 and NMR-1 are required for UNC-43 T284 phosphorylation in response to MSP, placing

these two receptors between MSP and UNC-43 in the signaling hierarchy (Fig. 5B). Binding studies support a direct interaction between MSP and VAB-1 (Miller et al., 2003), but not MSP and NMR-1. Therefore, we favor a model in which MSP binding to VAB-1 initiates a transduction process resulting in NMR-1-dependent UNC-43 activation (Fig. 5B), although we cannot exclude the possibility that another MSP receptor is involved. Further support for this model comes from studies of the sheath contraction mechanism, which does not require ephrin signaling. MSP induces *unc-43* activation in sheath cells to attenuate the basal contraction rate. Genetic analysis indicates that this response requires *vab-1* and *nmr-1*. *unc-43* is epistatic to mutations in *nmr-1*, a result consistent with the idea that UNC-43 acts downstream of NMR-1. From maturation and contraction data, we infer that VAB-1 and NMR-1 act in a positive direction to promote UNC-43 T284 phosphorylation and signaling. When sperm are absent from the reproductive tract, VAB-1 and NMR-1 act in the germline as negative regulators of meiotic maturation. Collectively, the data support the hypothesis that VAB-1 switches from a negative regulator into a redundant positive regulator of maturation upon binding to MSP. NMR-1 mediates this switch by controlling UNC-43 activation at the cortex (Fig. 5). Once activated, UNC-43 stimulates oocyte MPK-1 MAPK activation and meiotic maturation, either indirectly by downregulating ephrin/VAB-1- and CEH-18-dependent inhibition or by a more direct mechanism (not shown in Fig. 5B).

Clues regarding the biochemical mechanism by which VAB-1 and NMR-1 pathways control oocyte maturation come from studies of the mammalian central nervous system. NMDA receptors and CaMKII are integrally involved in synaptic plasticity and they directly interact in cultured cells (Bayer et al., 2001; Lisman and McIntyre, 2001). EphB receptor activation induces a direct interaction with NMDA receptors, resulting in the recruitment of CaMKII (Dalva et al., 2000). Our results are consistent with the possibility that VAB-1, NMR-1 and UNC-43 are components of a heteromeric complex located at the oocyte surface. Two genes encoding proteins implicated in organizing and trafficking RPTK signaling complexes, caveolin (*cav-1*) and tetraspanin (*tsp-12*), are required to negatively regulate oocyte maturation and MAPK activation (Miller et al., 2004). We speculate that an interactive network of negative and positive regulators functions at the oocyte cortex, possibly in multiprotein complexes, to control meiotic maturation rates in response to fluctuating concentrations of MSP.

Coordinating responses and generating signaling specificity

RPTK activation at the cell surface can result in a variety of tissue specific-responses. However, many of these responses are mediated by common downstream pathways, such as the Ras/MAPK and phospholipase Cγ/IP$_3$ cascades. MSP stimulates parallel responses in oocytes and ovarian sheath cells to ensure that oocyte maturation, ovulation and fertilization are tightly coupled. To coordinate these responses, MSP binds to the VAB-1 Eph RPTK on oocyte and sheath surfaces. Our results, together with those from previous studies, indicate that NMR-1 NMDA and ITR-1 IP$_3$ receptors act downstream of MSP in both cell types (Yin et al., 2004) (M.A.M., unpublished). These pathways regulate meiotic

maturation in oocytes and smooth muscle-like contraction in sheath cells. NMDA and IP$_3$ receptors mobilize intracellular Ca^{2+}, which is a ubiquitous second messenger that can regulate the cell cycle and cytoskeleton, depending on the Ca^{2+}-responsive effectors that are present in a given cell. The parallel structure of the MSP transduction mechanism allows oocytes and sheath cells to respond differently to the same stimulus with minimal genetic complexity.

Specificity in signaling can be achieved through the activation of distinct downstream effectors. The cyclin-dependent kinase CDK-1 and polo-like kinase PLK-1 are two downstream mediators of oocyte maturation in *C. elegans* (Boxem et al., 1999; Chase et al., 2000). The actin-linked regulators tropomyosin and troponin probably function in the sheath cells to regulate contraction (Ono and Ono, 2004). Therefore, Ca^{2+} mobilization acts upstream of CDK-1 and PLK-1 in oocytes and tropomyosin and troponin in sheath cells. *itr-1* acts downstream of the *let-23* EGF RPTK homolog in the spermatheca to control valve dilation during ovulation (Clandinin et al., 1998; Ono and Ono, 2004). Taken together, RPTK activation of the phospholipase Cγ/IP$_3$ pathway regulates oocyte meiotic maturation, ovarian sheath contraction and spermathecal valve dilation. These opposing cell types must be programmed to respond differently to Ca^{2+} mobilization. The collective action of shared RPTK signaling cascades and cell type-specific effectors is predicted to help drive fertilization in the *C. elegans* gonad.

Supplementary material
Supplementary material for this article is available at
http://dev.biologists.org/cgi/content/full/132/23/5225/DC1

References

Barton, M. K., Schedl, T. B. and Kimble, J. (1987). Gain-of-function mutations of fem-3, a sex-determination gene in Caenorhabditis elegans. *Genetics* **115**, 107-119.
Bayer, K. U., De Koninck, P., Leonard, A. S., Hell, J. W. and Schulman, H. (2001). Interaction with the NMDA receptor locks CaMKII in an active conformation. *Nature* **411**, 801-805.
Baylis, H. A., Furuichi, T., Yoshikawa, F., Mikoshiba, K. and Sattelle, D. B. (1999). Inositol 1,4,5-trisphosphate receptors are strongly expressed in the nervous system, pharynx, intestine, gonad and excretory cell of Caenorhabditis elegans and are encoded by a single gene (itr-1). *J. Mol. Biol.* **294**, 467-476.
Berridge, M. J. (1993). Inositol trisphosphate and calcium signalling. *Nature* **361**, 315-325.
Bottino, D., Mogilner, A., Roberts, T., Stewart, M. and Oster, G. (2002). How nematode sperm crawl. *J. Cell Sci.* **115**, 367-384.
Boxem, M., Srinivasan, D. G. and van den Heuvel, S. (1999). The Caenorhabditis elegans gene ncc-1 encodes a cdc2-related kinase required for M phase in meiotic and mitotic cell divisions, but not for S phase. *Development* **126**, 2227-2239.
Brenner, S. (1974). The genetics of Caenorhabditis elegans. *Genetics* **77**, 71-94.
Brockie, P. J., Mellem, J. E., Hills, T., Madsen, D. M. and Maricq, A. V.

(2001). The C. elegans glutamate receptor subunit NMR-1 is required for slow NMDA-activated currents that regulate reversal frequency during locomotion. *Neuron* **31**, 617-630.

Chase, D., Serafinas, C., Ashcroft, N., Kosinski, M., Longo, D., Ferris, D. K. and Golden, A. (2000). The polo-like kinase PLK-1 is required for nuclear envelope breakdown and the completion of meiosis in Caenorhabditis elegans. *Genesis* **26**, 26-41.

Chin-Sang, I. D., George, S. E., Ding, M., Moseley, S. L., Lynch, A. S. and Chisholm, A. D. (1999). The ephrin VAB-2/EFN-1 functions in neuronal signaling to regulate epidermal morphogenesis in C. elegans. *Cell* **99**, 781-790.

Clandinin, T. R., DeModena, J. A. and Sternberg, P. W. (1998). Inositol trisphosphate mediates a RAS-independent response to LET-23 receptor tyrosine kinase activation in C. elegans. *Cell* **92**, 523-533.

Colbran, R. J. (2004). Targeting of calcium/calmodulin-dependent protein kinase II. *Biochem. J.* **378**, 1-16.

Dal Santo, P., Logan, M. A., Chisholm, A. D. and Jorgensen, E. M. (1999). The inositol trisphosphate receptor regulates a 50-second behavioral rhythm in C. elegans. *Cell* **98**, 757-767.

Dalva, M. B., Takasu, M. A., Lin, M. Z., Shamah, S. M., Hu, L., Gale, N. W. and Greenberg, M. E. (2000). EphB receptors interact with NMDA receptors and regulate excitatory synapse formation. *Cell* **103**, 945-956.

Detwiler, M. R., Reuben, M., Li, X., Rogers, E. and Lin, R. (2001). Two zinc finger proteins, OMA-1 and OMA-2, are redundantly required for oocyte maturation in C. elegans. *Dev. Cell* **1**, 187-199.

Ellis, R. E. and Kimble, J. (1995). The fog-3 gene and regulation of cell fate in the germ line of Caenorhabditis elegans. *Genetics* **139**, 561-577.

Eppig, J. J. (2001). Oocyte control of ovarian follicular development and function in mammals. *Reproduction* **122**, 829-838.

Hall, D. H., Winfrey, V. P., Blaeuer, G., Hoffman, L. H., Furuta, T., Rose, K. L., Hobert, O. and Greenstein, D. (1999). Ultrastructural features of the adult hermaphrodite gonad of Caenorhabditis elegans: relations between the germ line and soma. *Dev. Biol.* **212**, 101-123.

Hassold, T. and Hunt, P. (2001). To err (meiotically) is human: the genesis of human aneuploidy. *Nat. Rev. Genet.* **2**, 280-291.

Hill, K. L. and L'Hernault, S. W. (2001). Analyses of reproductive interactions that occur after heterospecific matings within the genus Caenorhabditis. *Dev. Biol.* **232**, 105-114.

Hook, S. S. and Means, A. R. (2001). Ca(2+)/CaM-dependent kinases: from activation to function. *Annu. Rev. Pharmacol. Toxicol.* **41**, 471-505.

Hubbard, E. J. and Greenstein, D. (2000). The Caenorhabditis elegans gonad: a test tube for cell and developmental biology. *Dev. Dyn.* **218**, 2-22.

Hunt, P. A. and LeMaire-Adkins, R. (1998). Genetic control of mammalian female meiosis. *Curr. Top. Dev. Biol.* **37**, 359-381.

Kamath, R. S., Fraser, A. G., Dong, Y., Poulin, G., Durbin, R., Gotta, M., Kanapin, A., Le Bot, N., Moreno, S., Sohrmann, M. et al. (2003). Systematic functional analysis of the Caenorhabditis elegans genome using RNAi. *Nature* **421**, 231-237.

Kosinski, M., McDonald, K., Schwartz, J., Yamamoto, I. and Greenstein, D. (2005). C. elegans sperm bud vesicles to deliver a meiotic maturation signal to distant oocytes. *Development* **132**, 3357-3369.

Kroiher, M., Miller, M. A. and Steele, R. E. (2001). Deceiving appearances: signaling by 'dead' and 'fractured' receptor protein-tyrosine kinases. *BioEssays* **23**, 69-76.

Lisman, J. E. and McIntyre, C. C. (2001). Synaptic plasticity: a molecular memory switch. *Curr. Biol.* **11**, R788-R791.

Marston, D. J., Dickinson, S. and Nobes, C. D. (2003). Rac-dependent trans-endocytosis of ephrinBs regulates Eph-ephrin contact repulsion. *Nat. Cell Biol.* **5**, 879-888.

Masui, Y. (1985). Meiotic arrest in animal oocytes. In *Biology of Fertilization*, Vol. 1 (ed. A. Monroy and C. B. Metz), pp. 189-219. Orlando, FL: Academic Press.

Masui, Y. and Clarke, H. J. (1979). Oocyte maturation. *Int. Rev. Cytol.* **57**, 185-282.

McCarter, J., Bartlett, B., Dang, T. and Schedl, T. (1999). On the control of oocyte meiotic maturation and ovulation in Caenorhabditis elegans. *Dev. Biol.* **205**, 111-128.

Miller, M. A., Nguyen, V. Q., Lee, M. H., Kosinski, M., Schedl, T., Caprioli, R. M. and Greenstein, D. (2001). A sperm cytoskeletal protein that signals oocyte meiotic maturation and ovulation. *Science* **291**, 2144-2147.

Miller, M. A., Ruest, P. J., Kosinski, M., Hanks, S. K. and Greenstein, D. (2003). An Eph receptor sperm-sensing control mechanism for oocyte meiotic maturation in Caenorhabditis elegans. *Genes Dev.* **17**, 187-200.

Miller, M. A., Cutter, A. D., Yamamoto, I., Ward, S. and Greenstein, D.

(2004). Clustered organization of reproductive genes in the C. elegans genome. *Curr. Biol.* **14**, 1284-1290.

Ono, K. and Ono, S. (2004). Tropomyosin and troponin are required for ovarian contraction in the Caenorhabditis elegans reproductive system. *Mol. Biol. Cell* **15**, 2782-2793.

Papp, B., Pal, C. and Hurst, L. D. (2003). Dosage sensitivity and the evolution of gene families in yeast. *Nature* **424**, 194-197.

Pasquale, E. B. (2005). Eph receptor signalling casts a wide net on cell behaviour. *Nat. Rev. Mol. Cell. Biol.* **6**, 462-475.

Pincus, G. and Enzmann, E. V. (1935). The comparative behaviour of mammalian eggs *in vivo* and *in vitro*. *J. Exp. Med.* **62**, 655-675.

Poliakov, A., Cotrina, M. and Wilkinson, D. G. (2004). Diverse roles of eph receptors and ephrins in the regulation of cell migration and tissue assembly. *Dev. Cell* **7**, 465-480.

Reiner, D. J., Newton, E. M., Tian, H. and Thomas, J. H. (1999). Diverse behavioral defects caused by mutations in Caenorhabditis elegans unc-43 CaM kinase II. *Nature* **402**, 199-203.

Rose, K. L., Winfrey, V. P., Hoffman, L. H., Hall, D. H., Furuta, T. and Greenstein, D. (1997). The POU gene ceh-18 promotes gonadal sheath cell differentiation and function required for meiotic maturation and ovulation in Caenorhabditis elegans. *Dev. Biol.* **192**, 59-77.

Schedl, T. and Kimble, J. (1988). fog-2, a germ-line-specific sex determination gene required for hermaphrodite spermatogenesis in Caenorhabditis elegans. *Genetics* **119**, 43-61.

Sijen, T., Fleenor, J., Simmer, F., Thijssen, K. L., Parrish, S., Timmons, L., Plasterk, R. H. and Fire, A. (2001). On the role of RNA amplification in dsRNA-triggered gene silencing. *Cell* **107**, 465-476.

Timmons, L. and Fire, A. (1998). Specific interference by ingested dsRNA. *Nature* **395**, 854.

Wang, X., Roy, P. J., Holland, S. J., Zhang, L. W., Culotti, J. G. and Pawson, T. (1999). Multiple ephrins control cell organization in C. elegans using kinase-dependent and -independent functions of the VAB-1 Eph receptor. *Mol. Cell* **4**, 903-913.

Ward, S. and Carrel, J. S. (1979). Fertilization and sperm competition in the nematode Caenorhabditis elegans. *Dev. Biol.* **73**, 304-321.

Yin, X., Gower, N. J., Baylis, H. A. and Strange, K. (2004). Inositol 1,4,5-trisphosphate signaling regulates rhythmic contractile activity of myoepithelial sheath cells in Caenorhabditis elegans. *Mol. Biol. Cell* **15**, 3938-3949.

Yoshikawa, F., Morita, M., Monkawa, T., Michikawa, T., Furuichi, T. and Mikoshiba, K. (1996). Mutational analysis of the ligand binding site of the inositol 1,4,5-trisphosphate receptor. *J. Biol. Chem.* **271**, 18277-18284.